

Influence of disorder on incoherent transport near the Mott transition

Miloš M. Radonjić,¹ D. Tanasković,¹ V. Dobrosavljević,² and K. Haule³

¹*Scientific Computing Laboratory, Institute of Physics Belgrade, Pregrevica 118, 11080 Belgrade, Serbia*

²*Department of Physics and National High Magnetic Field Laboratory,
Florida State University, Tallahassee, Florida 32306, USA*

³*Department of Physics and Astronomy, Rutgers University, Piscataway, New Jersey 08854, USA*

We calculate the optical and DC conductivity for half-filled disordered Hubbard model near the Mott metal-insulator transition. As in the clean case, large metallic resistivity is driven by a strong inelastic scattering, and Drude-like peak in the optical conductivity persists even at temperatures when the resistivity is well beyond the semiclassical Mott-Ioffe-Regel limit. Local random potential does not introduce new charge carriers, but it induces effective local carrier doping and broadens the bandwidth. This makes the system more metallic, in agreement with the recent experiments on X-ray irradiated charge-transfer salts.

PACS numbers: 71.10.Fd, 71.30.+h, 72.15.Qm

I. INTRODUCTION

Thermodynamic and transport properties of many strongly correlated materials are influenced by inhomogeneities and disorder,¹ and their importance becomes even more evident with the advances in experimental techniques.^{2,3} Very recently, the effects of disorder on the optical and DC conductivity of the organic charge-transfer salts have been systematically explored by introducing defects by X-ray irradiation.⁴⁻⁶ The conductivity has proven to be very sensitive on the duration of the irradiation, and different physical mechanisms were advocated to explain such a behavior.⁴⁻⁶

Members of κ -family of organic charge-transfer salts have half-filled conduction bands with the effective Coulomb repulsion comparable to the bandwidth,⁷ and their proximity to the Mott metal-insulator transition can be tuned by doping or applying the pressure. On the metallic side of the Mott transition, the Fermi liquid transport at low temperatures is followed by an incoherent transport at higher temperatures dominated by the large scattering rate, and with resistivities an order of magnitude larger than the Mott-Ioffe-Regel (MIR) limit,⁸⁻¹² which is the maximal resistivity that can be reached in a metal according to the Boltzmann semiclassical theory. From the theoretical point of view, the violation of the MIR condition and the appearance of the maximum in the resistivity temperature dependence is not easy to explain. However, at least for κ -organics, a significant progress has been recently achieved when the transport properties were successfully described even on the quantitative level within the dynamical mean field theory (DMFT).¹³⁻¹⁵ Therefore, it is important to explore the effects of X-ray irradiation within the same theoretical framework by introducing the disorder into the model.

Most of the theoretical work on the influence of disorder on the physical properties near the Mott transition have been so far restricted to binary disorder distribution,¹⁶ or low temperatures where the DMFT

has been extended in order to incorporate the Anderson localization effects.¹⁷⁻¹⁹ However, for a comparison with the experiments on κ -organics, we need the results in a wide temperature range, and since the disorder is gradually generated by X-ray irradiation, the simplest approach of disorder averaging on the level of coherent-potential approximation (CPA),²⁰ that we apply in our work, should be sufficient to explain the main modifications in the optical and DC conductivity caused by the disorder. We find that, as in the clean case, it is the large electron-electron scattering that leads to the destruction of coherent quasiparticles and to the resistivity well beyond the MIR limit on the metallic side of the Mott transition. For a fixed interaction strength, however, the random potential effectively weakens the correlation effects and moves the system away from the Mott transition. Therefore, the disorder increases the conductivity in agreement with the experiments on the organic charge-transfer salts.

The rest of the paper is organized as follows. Section II contains the DMFT equations for the disordered Hubbard model, brief discussion on the impurity solvers that we use and comments on the validity of the DMFT approximation. Section III presents the results for the temperature dependence of the density of states, optical conductivity and DC resistivity near the Mott transition for the pure and disordered system. Our results are compared with the experiments on X-ray irradiated κ -organics in Section IV. Section V contains the conclusions.

II. DISORDERED HUBBARD MODEL

We consider half-filled Hubbard model with site-diagonal disorder as given by the Hamiltonian

$$H = - \sum_{ij,\sigma} t_{i,j} c_{i\sigma}^\dagger c_{j\sigma} + U \sum_i n_{i\uparrow} n_{i\downarrow} + \sum_{i\sigma} v_i n_{i\sigma} - \mu \sum_{i\sigma} n_{i\sigma}. \quad (2.1)$$

Here $t_{i,j}$ is the hopping amplitude, U the interaction strength, $c_{i\sigma}^\dagger$ is the creation operator, and $n_{i\sigma} = c_{i\sigma}^\dagger c_{i\sigma}$ the occupation number operator on site i and for spin σ . Half-filling condition is enforced by the chemical potential μ . We model the disorder by random energies v_i taken from the uniform distribution in the interval $(-W/2, W/2)$.

In the dynamical mean field theory, which is formally exact in the limit of large coordination number, the Hubbard model reduces to a model of an Anderson impurity in a conduction bath which has to be determined self-consistently. In the presence of disorder, we need to consider an ensemble of impurities, and the conduction bath is determined in the process of averaging over the disorder.

The central quantity in DMFT is the local Green function, $G_{i\sigma}(\tau - \tau') = -\langle T c_{i\sigma}(\tau) c_{i\sigma}^\dagger(\tau') \rangle_{S_{eff}^i}$, which is a site-dependent quantity in the presence of disorder. The local effective action is given by

$$S_{eff}^i = -\frac{1}{\beta} \sum_{i\omega_n, \sigma} c_{i\sigma}^\dagger(i\omega_n) [i\omega_n + \mu - v_i - \Delta(i\omega_n)] c_{i\sigma}(i\omega_n) + \frac{1}{\beta} U \sum_{i\omega_n} n_\uparrow(i\omega_n) n_\downarrow(i\omega_n), \quad (2.2)$$

where Δ is the conduction bath whose self-consistent value will be obtained in the iterative procedure. The quantity that we average over the disorder is the local Green function, $G_{av}(i\omega_n) = \int dv P(v) G(i\omega_n, v)$. Though we consider a continuous distribution of disorder, $P(v)$, in practice it is sufficient to take a finite number of random energies, and the integral replaces with a sum. In the case of uniform disorder

$$G_{av}(i\omega_n) = \frac{1}{N} \sum_{i=1}^N G_i(i\omega_n). \quad (2.3)$$

The averaged Green function G_{av} and the conduction bath Δ determine the self-energy through the relation

$$G_{av}^{-1}(i\omega_n) = i\omega_n + \mu - \Delta(i\omega_n) - \Sigma(i\omega_n). \quad (2.4)$$

The self-consistency condition follows from the assumption that the lattice self-energy coincides with the impurity self-energy. Then the disorder averaged local Green function has to be equal to the local component of the lattice Green function,

$$G_{av}(i\omega_n) = \int d\varepsilon \frac{D(\varepsilon)}{i\omega_n + \mu - \varepsilon - \Sigma(i\omega_n)}. \quad (2.5)$$

Here $D(\varepsilon)$ is the density of states in the absence of disorder and interaction. Eq. (2.4) determines new conduction bath which completes the self-consistency loop. We note that our treatment of disorder reduces to the CPA approximation in the absence of interaction.

The most difficult step in the solution of DMFT equation is the calculation of the local Green function from

the Anderson impurity action Eq. (2.2). In this paper, we solve the Anderson impurity model with One-Crossing Approximation (OCA),^{21,22} and cross-check the results with Continuous Time Quantum Monte Carlo (CTQMC) impurity solver.^{23,24} The OCA impurity solver has an advantage that it gives a solution on real frequency axis, which is necessary for a calculation of the response functions. Except at the lowest temperatures, where the OCA impurity solver does not reproduce the Fermi-liquid behavior, the results obtained with these two impurity solvers are qualitatively the same and quantitatively very similar.

Since we are going to compare the results with the experiments on κ -organics, we briefly comment on the validity of DMFT approximation. The main advantage of this method is that it treats on an equal footing low and high energy part of the spectrum and fully takes into account the inelastic electron-electron scattering. Therefore, it successfully describes a crossover from the low temperature Fermi liquid regime to the incoherent transport at higher temperatures, which is typical for many strongly correlated systems. The DMFT is based on the assumption of locality of the self-energy, and hence it does not fully take into account intersite correlations. However, the κ -organics have weakly anisotropic triangular lattice structure⁷ which makes the intersite correlations smaller due to the geometrical frustration. In this case, local DMFT approximation gives similar results as generalized cluster DMFT.²⁵ Finally, since the lattice structure enters the DMFT equations only through the density of states, the transport properties does not depend much on the details of the band structure, and we will consider the hypercubic lattice which has the density of states in the form of a Gaussian $D(\varepsilon) = \sqrt{\frac{2}{\pi}} e^{-2\varepsilon^2}$, where the energy is given in units of the half-bandwidth.

III. CONDUCTIVITY NEAR THE MOTT TRANSITION

The phase diagram of half-filled Hubbard model in DMFT approximation is well known.²⁶ At low temperatures, an increase of the interaction U leads to the first order metal-insulator transition. The line of the first order phase transition ends in the critical point at temperature T_c and interaction U_c . In this work we will concentrate on the values of interaction equal and slightly lower than U_c . At these values of U , there is a gradual crossover from the Fermi liquid to an incoherent metallic and, eventually, insulating behavior as the temperature is increased.

The central quantity that we calculate is the optical conductivity. In DMFT it is given by²⁶

$$\sigma(\omega) = \frac{\pi e^2}{\hbar} \int_{-\infty}^{+\infty} d\varepsilon \int_{-\infty}^{+\infty} d\nu D(\varepsilon) \rho(\varepsilon, \nu) \rho(\varepsilon, \nu + \omega) \times \frac{f(\nu) - f(\nu + \omega)}{\omega}. \quad (3.1)$$

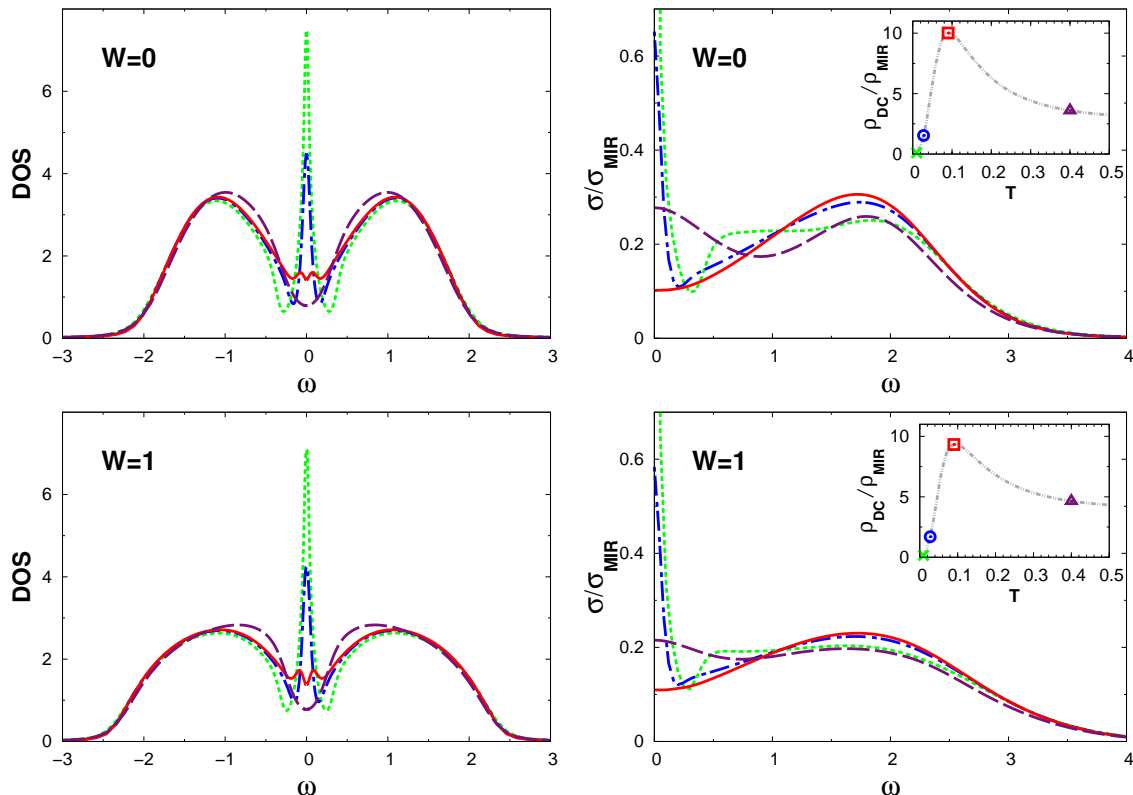


FIG. 1: (Color online) Density of states and optical conductivity as a function of frequency in the clean case for $U = 0.94 U_c|_{W=0}$ (upper panel) and disordered case, $U = 0.94 U_c|_{W=1}$ (lower panel). Different colors correspond to the four distinctive transport regimes (see the text). The insets show the temperature dependence of DC resistivity. T , ω and W are given in units of bare E_F .

Here $\rho(\epsilon, \nu) = -\frac{1}{\pi} \text{Im}G(\epsilon, \nu)$, and $G(\epsilon, \nu) = (\nu + \mu - \epsilon - \Sigma(\nu))^{-1}$. We will express the conductivity in units of the Mott-Ioffe-Regel limit for minimal metallic conductivity. The MIR limit, σ_{MIR} , is the conductivity which is reached when the electron mean free path becomes comparable to the lattice spacing, $l \sim a$. According to the semiclassical arguments, the electrons can scatter at most on every atom and the conductivity in a metal cannot be smaller than σ_{MIR} . For half-filled hypercubic lattice (which has Gaussian density of states), the MIR condition $l = a$ is equivalent to $E_F \tau = 1$, where E_F is the bare Fermi energy, i.e. half-bandwidth of the noninteracting electrons, and τ^{-1} is the scattering rate. Here \hbar is set to 1. Therefore, the MIR limit is set by a condition

$$\tau_{MIR}^{-1} = -2\text{Im}\Sigma(0^+) = 1, \quad (3.2)$$

where Σ is the self-energy measured in units of E_F .

The density of states and optical conductivity for a clean system and in a presence of moderate disorder, $W = 1$, are shown in Fig. 1. The disorder effectively increases the bandwidth and the critical interaction U_c . In our case, we find that $U_c|_{W=0} = 2.2$ and $U_c|_{W=1} = 2.45$. The increase of U_c due to disorder is in agreement with earlier estimates obtained by iterated perturbation

theory.²⁷ The critical temperature T_c weakly depends on the disorder strength, $T_c|_{W=1} \approx T_c|_{W=0} = 0.04$, where k_B is set to 1. On Fig. 1 we compare the data at the same relative value $U/U_c = 0.94$, and for several characteristic temperatures. We see that the disorder does not lead to qualitative differences and if the interaction is the same when scaled with U_c , the density of states and the optical conductivity are even quantitatively very similar.

We can identify several regimes of the electron transport. At low temperature (green dotted lines and crosses in the insets) the scattering rate, $\tau^{-1} = -2\text{Im}\Sigma(0^+)$, is small and the transport is dominated by long-lived coherently propagating quasiparticles. The blue dash-dotted lines (blue circles in the insets) correspond to the temperature when the resistivity is already larger than the MIR limit, the scattering rate τ^{-1} is larger than E_F , and the Fermi liquid picture of well-defined quasiparticles ceases to be valid. However, a Drude-like peak in the optical conductivity, as well as a peak in the density of states, are still present. Our results show that this is the case also in the presence of moderate disorder. The resistivity maximum (red full line and square) is reached when the peak at the Fermi level is fully suppressed and when a dip at the Fermi level appears both in

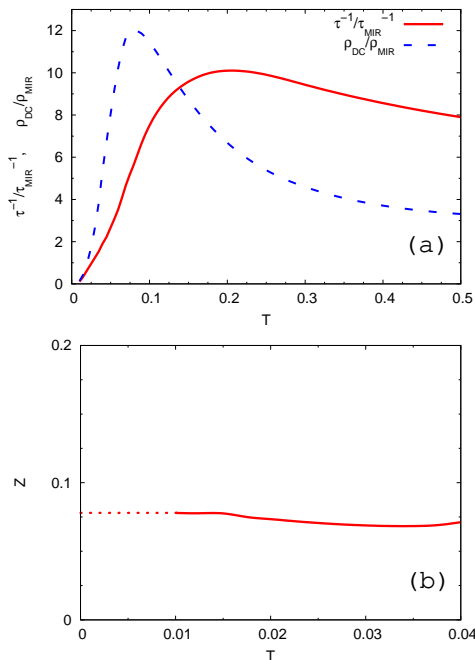


FIG. 2: (Color online) (a) Scattering rate (full line) and DC resistivity (dashed) as a function of temperature. (b) Quasiparticle weight as a function of temperature. The data are for the clean system at $U = 0.95 U_c$.

the density of states and in the optical conductivity. The resistivity maximum is more than an order of magnitude larger than $\rho_{MIR} = \sigma_{MIR}^{-1}$. At even higher temperatures (violet dashed line and triangle) low frequency optical conductivity increases due to the thermal excitations.

Fig. 2 helps us to further distinguish the mechanism leading to the large resistivity and its strong temperature dependence. We see that the scattering rate gives the main contribution to the resistivity temperature dependence and causes the violation of the MIR limit, Fig. 2(a), while the quasiparticle (Drude) weight $Z = (1 + |\partial \text{Re} \Sigma(\omega)/\partial \omega|_{\omega=0})^{-1}$ is almost temperature independent, Fig. 2(b). The dotted part of the line is an extrapolation of the OCA results to zero temperature. We have also checked that Z depends very weakly on the temperature using numerically exact CTQMC impurity solver. Therefore, we can conclude that the driving mechanism for large resistivity is the large scattering rate and not the reduction of the spectral weight near the Fermi level. This feature, already seen in the experiments on VO_2 ²⁸ and charge-transfer salts,¹⁵ seem to be common for the systems with half-filled conduction band near the Mott transition. This should be contrasted with the doped Mott insulators where the main reason for the violation of the MIR condition is a decimation of the Drude peak in the optical conductivity by the time MIR limit is reached, which can be interpreted as a reduction of the number of charge carriers.^{8,12}

The results for temperature dependence of DC resistiv-

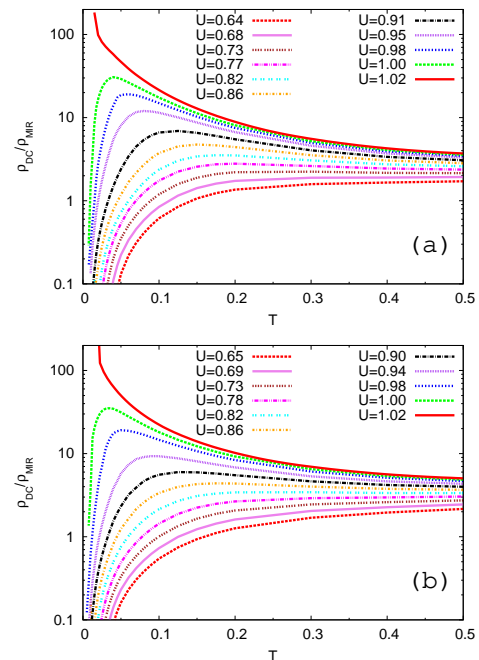


FIG. 3: (Color online) Temperature dependence of DC resistivity for different interaction U in the clean case, $W = 0$ (a) and disordered case, $W = 1$ (b). U is given in units of $U_c(W)$.

ity, $\rho_{DC} = \sigma^{-1}(\omega \rightarrow 0)$, for several values of interaction U are shown in Fig. 3. The resistivity is given in units ρ_{MIR} . For clarity it is shown on a logarithmic scale. The resistivity in the clean and disordered case are even quantitatively very similar when the interaction is scaled with $U_c(W)$.

IV. INCREASE OF METALLICITY BY DISORDER

Very recent experiments⁴⁻⁶ on the charge-transfer organic salts provide a rather unique opportunity to study the effects of disorder on transport properties without changing external parameters or chemical composition. The level of defects (disorder) directly depends on the time of exposure to the X-rays. The optical and DC conductivity are proven to be very sensitive on irradiation time showing an increase in the conductivity with the time of irradiation. The experiments measured both interlayer and in-plane resistivity with similar conclusions. Different physical mechanisms were proposed to explain the increase of conductivity. Analytis *et al.*⁴ proposed a defect-assisted interlayer conduction channel for the reduction of resistivity, and Sasaki *et al.*^{5,6} proposed that the irradiation leads to the effective doping of carriers into the half-filled Mott insulator.

The DMFT has successfully described the transport properties of organic salts even on the quantitative level.^{14,15} In order to make a comparison with the ex-

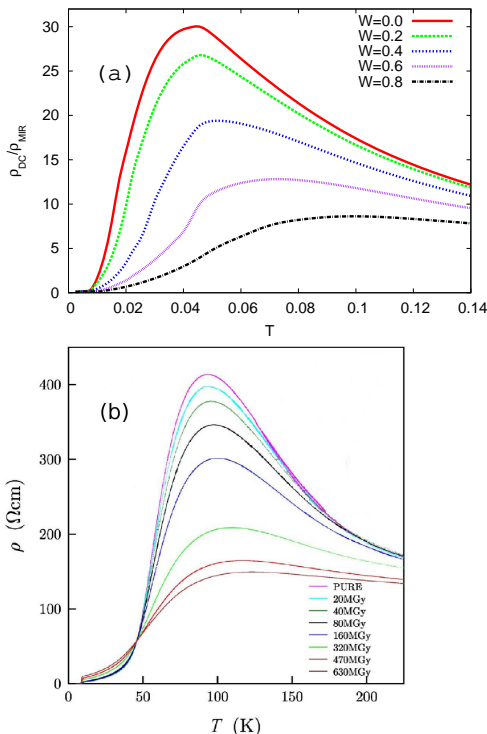


FIG. 4: (Color online) (a) Temperature dependence of DC resistivity for fixed $U = 2.2 = U_c|_{W=0}$, and various levels of disorder. (b) Experiments on κ -(BEDT-TTF) $_2$ Cu(SCN) $_2$, taken from Ref. 4.

periments with irradiation induced defects, we solve the DMFT equations for fixed interaction U and vary the level of disorder W . The results for DC resistivity are shown in Fig. 4(a). The data for $T < 0.01$ are obtained using CTQMC impurity solver. The presence of even a weak disorder significantly decreases the resistivity by effectively moving the system away from the Mott insulator, as explained in the previous section. Our data are very similar to the measurements on charge-transfer salt κ -(BEDT-TTF) $_2$ Cu(SCN) $_2$ from Ref. 4, which are shown in Fig. 4(b). We note that these data are for interlayer resistivity while our DMFT calculation corresponds to in-plane transport. However, the interlayer transport is due to incoherent tunneling which is proportional to in-plane conductivity.²⁹ Therefore the temperature dependence of out-of-plane resistivity should follow the temperature dependence of in-plane resistivity. Indeed, the in-plane optical conductivity measurements on the Mott insulator κ -(BEDT-TTF) $_2$ Cu[N(CN) $_2$]Cl, also show that the Mott system becomes more metallic in a presence of disorder. These measurements show the transfer of the spectral weight to low frequency region as the irradiation time increases, followed by the collapse of the Mott gap.^{5,6}

We emphasize that our model, as opposed to the physical mechanism proposed in Ref. 6, does not assume an introduction of new charge carriers since the total num-

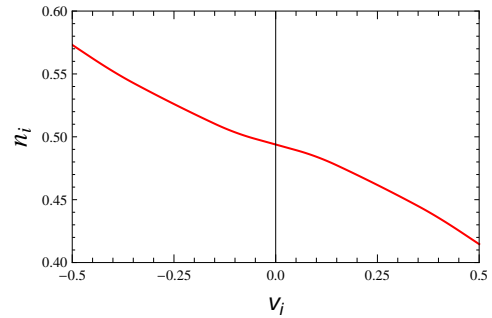


FIG. 5: (Color online) Local occupation number per spin as a function of site disorder v_i for $T = 0.01$, $U = 2.1$, and $W = 1$.

ber of carriers per site remains equal to one. The local occupation number, however, depends on the random site potential, and we can say that the system is effectively locally doped.³⁰ The occupation number, for a given spin orientation, as a function of random site potential is shown on Fig. 5. It is interesting to note that the local occupation number, $n(v_i)$, deviates much less from its average value than it would be the case in the absence of interaction. This is a consequence of very strong disorder screening of site-diagonal disorder on the metallic side of the Mott transition.³¹ Therefore, the resistivity curves on Fig. 4(a) cross at very low temperatures and our current model cannot explain the intersection of curves in Fig. 4(b) which happens at much higher temperature. The dramatic reduction of the elastic scattering is also demonstrated in Ref. 32, which shows that the inelastic scattering dominates in the incoherent regime. We stress that we do not assume Matthiessen's rule. This is a salient feature of DMFT, which can operate in a regime where conventional approaches to the electron transport fail.

V. CONCLUSIONS

In summary, we have examined the influence of random potential on the optical and DC conductivity for half-filled Hubbard model in a vicinity of the Mott transition. Our results show, in agreement with the experiments on κ -organics, that the disorder can make the system effectively more metallic. The disorder increases the bandwidth which increases U_c and weakens the correlation effects, moves the system away from the Mott transition and leads to a decrease in the scattering rate and resistivity. We emphasize that the randomness in our model does not change global doping, as the system remains on average half-filled, but the number of charge carriers locally deviates from the average value. Therefore, global carrier doping of a Mott insulator due to irradiation defects, proposed in Ref. 6, is not necessary to make the system more metallic. We also find that the maximal possible value of metallic resistivity remains more than

an order of magnitude larger than the MIR limit even in a presence of moderate disorder. As in the clean case, the violation of the MIR limit is driven by a large scattering rate due to the electron-electron scattering, and Drude-like peak in the optical conductivity persists even at temperatures when the resistivity is well beyond the MIR limit.

Acknowledgments

The authors acknowledge fruitful discussions with D.N. Basov and N.E. Hussey. This work was supported

by the Serbian Ministry of Science and Technological Development under Project No. OI 141035 (M.R. and D.T.), the NSF under Grant No. DMR-0542026 (V.D.) and the NSF Grant No. DMR-0746395 (K.H). M.R. acknowledges support from the FP6 Center of Excellence grant CX-CMCS and D.T. support from the NATO Science for Peace and Security Programme Reintegration Grant No. EAP.RIG.983235. Numerical results were obtained on the AEGIS e-Infrastructure, supported in part by FP7 projects EGEE-III and SEE-GRID-SCI.

-
- ¹ E. Miranda and V. Dobrosavljević, Rep. Prog. Phys. **68**, 2337 (2005).
- ² M. M. Qazilbash, M. Brehm, B.-G. Chae, P.-C. Ho, G. O. Andreev, B.-J. Kim, S. J. Yun, A. V. Balatsky, M. B. Maple, F. Keilmann, et al., Science **318**, 1750 (2007).
- ³ Y. Kohsaka, C. Taylor, K. Fujita, A. Schmidt, C. Lupien, T. Hanaguri, M. Azuma, M. Takano, H. Eisaki, H. Takagi, et al., Science **315**, 1380 (2007).
- ⁴ J. G. Analytis, A. Ardavan, S. J. Blundell, R. L. Owen, E. F. Garman, C. Jeynes, and B. J. Powell, Phys. Rev. Lett. **96**, 177002 (2006).
- ⁵ T. Sasaki, H. Oizumi, N. Yoneyama, N. Kobayashi, and N. Toyota, J. Phys. Soc. Jpn. **76**, 123701 (2007).
- ⁶ T. Sasaki, N. Yoneyama, Y. Nakamura, N. Kobayashi, Y. Ikemoto, T. Moriwaki, and H. Kimura, Phys. Rev. Lett. **101**, 206403 (2008).
- ⁷ B. J. Powell and R. H. McKenzie, J. Phys.: Condens. Matter **18**, R827 (2006).
- ⁸ O. Gunnarsson, M. Calandra, and J. E. Han, Rev. Mod. Phys. **75**, 1085 (2003).
- ⁹ M. Calandra and O. Gunnarsson, Phys. Rev. Lett. **87**, 266601 (2001).
- ¹⁰ M. Calandra and O. Gunnarsson, Phys. Rev. B **66**, 205105 (2002).
- ¹¹ M. B. Allen, Physica B **318**, 24 (2002).
- ¹² N. E. Hussey, K. Takenaka, and H. Takagi, Philos. Mag. **84**, 2847 (2004).
- ¹³ J. Merino and R. H. McKenzie, Phys. Rev. B **61**, 7996 (2000).
- ¹⁴ P. Limelette, P. Wzietek, S. Florens, A. Georges, T. A. Costi, C. Pasquier, D. Jérôme, C. Mézière, and P. Batail, Phys. Rev. Lett. **91**, 016401 (2003).
- ¹⁵ J. Merino, M. Dumm, N. Drichko, M. Dressel, and R. H. McKenzie, Phys. Rev. Lett. **100**, 086404 (2008).
- ¹⁶ M. S. Laad, L. Craco, and E. Müller-Hartmann, Phys. Rev. B **64**, 195114 (2001).
- ¹⁷ V. Dobrosavljević and G. Kotliar, Phys. Rev. Lett. **78**, 3943 (1997).
- ¹⁸ V. Dobrosavljević, A. A. Pastor, and B. K. Nikolić, Europhys. Lett. **62**, 76 (2003).
- ¹⁹ K. Byczuk, W. Hofstetter, and D. Vollhardt, Phys. Rev. Lett. **94**, 056404 (2005).
- ²⁰ E. N. Economou, *Greens Functions in Quantum Physics* (Springer, Berlin, 2005), 3rd ed.
- ²¹ T. Pruschke, D. L. Cox, and M. Jarrell, Phys. Rev. B **47**, 3553 (1993).
- ²² K. Haule, S. Kirchner, J. Kroha, and P. Wölfle, Phys. Rev. B **64**, 155111 (2001).
- ²³ P. Werner, A. Comanac, L. de Medici, M. Troyer, and A. J. Millis, Phys. Rev. Lett. **97**, 076405 (2006).
- ²⁴ K. Haule, Phys. Rev. B **75**, 155113 (2007).
- ²⁵ A. Liebsch, H. Ishida, and J. Merino, Phys. Rev. B **79**, 195108 (2009).
- ²⁶ A. Georges, G. Kotliar, W. Krauth, and M. J. Rozenberg, Rev. Mod. Phys. **68**, 13 (1996).
- ²⁷ M. C. Aguiar, V. Dobrosavljević, E. Abrahams, and G. Kotliar, Phys. Rev. B **71**, 205115 (2005).
- ²⁸ M. M. Qazilbash, K. S. Burch, D. Whisler, D. Shrekenhamer, B. G. Chae, H. T. Kim, and D. N. Basov, Phys. Rev. B **74**, 205118 (2006).
- ²⁹ R. H. McKenzie and P. Moses, Phys. Rev. Lett. **81**, 4492 (1998).
- ³⁰ D. Heidarian and N. Trivedi, Phys. Rev. Lett. **93**, 126401 (2004).
- ³¹ D. Tanasković, V. Dobrosavljević, E. Abrahams, and G. Kotliar, Phys. Rev. Lett. **91**, 066603 (2003).
- ³² M. C. Aguiar, E. Miranda, V. Dobrosavljević, E. Abrahams, and G. Kotliar, Europhys. Lett. **67**, 226 (2004).